2011 American Control Conference
on O'Farrell Street, San Francisco, CA, USA
June 29 - July 01, 2011

Collision Avoidance Norms In Trajectory Planning

Sujit Nair
Senior Scientist
United Technologies Research Center
East Hartford, CT 06118
NairSS@utrc.utc.com

Marin Kobilarov
Control & Dynamical Systems
California Institute of Technology
Pasadena, CA 91125
marin@cds.caltech.edu

Abstract— **This paper studies norms that quantify safety of robotic vehicle trajectories. The main motivation behind this work is to automate the process of selecting safe motions in complex state spaces such as ones arising from environments cluttered with obstacles or when trajectories lie close to the permitted boundary of configuration space. An autonomous vehicle can plan obstacle-free trajectories in a known environment but the inherent uncertainty in sensing and motion could render these trajectories unsafe during execution. Therefore, in the presence of uncertainty it is crucial to predict in real-time the *safety of planned trajectories* through appropriate metrics or norms. There are a number of standard methods to weigh risks associated with vehicle behavior, for instance, based on the minimum distance to the closest obstacles, or on the average distance to obstacles along the trajectory. In this paper we study generalization of such norms based on the theory of *Sobolev spaces*. In particular, H^k Sobolev norms applied to the distance-to-obstacle function along a trajectory are based not only on its spatial properties but also on its time variation or *frequency components*. We show that this extra information renders an H^1 norm more effective for quantifying risk compared to the standard L^p norms. This is demonstrated for an analytical example as well as for a semi-realistic helicopter flying through an obstacle terrain.**

I. INTRODUCTION

Obstacle avoidance is one of the classical and most well studied problems in robotics. Robotic vehicles operating in obstructed environments must plan and safely execute collision-free trajectories. Uncertainty in motion and sensing naturally present in most settings can potentially influence the executed trajectory and render it unsafe. The typical approach to deal with noise is through sensor-based navigation (see e.g. [1], [2]). Yet, quantifying the expected performance and safety during sensor-based execution is a difficult issue since it relies on precise knowledge of the vehicle and environment dynamics, and all sources of uncertainty present. Even if such information were available its proper use requires extensive simulations that sample the possible uncertain outcomes in the given time horizon. This paper does not consider such an approach for dealing with uncertainty. Instead, it is concerned with quantifying uncertainty heuristically based solely on the distance to known obstacles along the trajectory. While such information is limiting and does not provide guarantees for safety during execution, it leads to simple computations that can be used for real-time decision making. In essense, this paper poses the question: given a trajectory of a system with no information about the underlying uncertainty in sensing and motion model how to compute a single value (measure) quantifying safety based solely on distance to obstacles. This paper shows that a Sobolev norm (i.e. including temporal frequency components) measure provides a richer notion of safety than a standard euclidean norm (i.e. based on spatial components only).

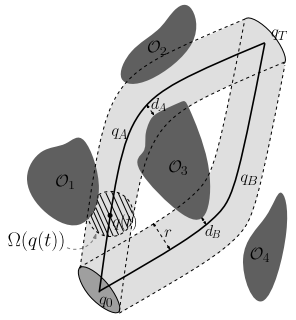

Fig. 1. Two trajectories of a vehicle (modeled here as a point for clarity) among obstacles.

Consider a situation (see Fig. 1) in which a robotic vehicle[1] navigates across a workspace denoted by $\mathcal{W}$, where $\mathcal{W} = \mathbb{R}^2$, or $\mathbb{R}^3$. Following standard notation (e.g. [3], [4]), let the configuration at time t be denoted by $q(t) \in \mathcal{C}$, where $\mathcal{C}$ is the configuration space, for instance describing the the position, orientation, and joint angles of the system. Assume that the vehicle is occupying a region $\mathcal{A}(q(t)) \subset \mathcal{W}$ and must travel from configuration $q_0 \in \mathcal{C}$ to configuration $q_T \in \mathcal{C}$ at time T while avoiding obstacles $\mathcal{O}_i \subset \mathcal{W}$. Equivalently, it is required that $q(t) \in \mathcal{C}_{free}$ for all $t \in [0, T]$, where $\mathcal{C}_{free} = \{q \mid \mathcal{A}(q) \cap \mathcal{O} = \emptyset\}$ with $\mathcal{O} = \{\mathcal{O}_1, \mathcal{O}_2, ...\}$ denoting the set of all obstacles. A vehicle is in collision whenever its configuration lies at the boundary of the free space, i.e. when $q \in \partial\mathcal{C}_{free}$. In addition, the closest distance between the vehicle and obstacles is defined by the function

$$d(q) = \min_{x,x'}\{\|x - x'\| \mid x \in \mathcal{A}(q), x' \in \mathcal{O}\}, \quad (1)$$

and the obstacle avoidance requirement can be expressed as $d(q) > 0$. The exact form of this function for almost any type of obstacle is well established (e.g. [3]).

The vehicle motion is subject to uncertainty and the actual executed trajectory is denoted by $\widetilde{q} : [0, T] \rightarrow \mathrm{cl}(\mathcal{C}_{free})$, where the closure operator applied to an open set X, $\mathrm{cl}(X) = X \cup \partial X$, simply closes the set by adding its

[1]The term "vehicle" refers to any mobile robotic system such as wheeled robot, an aerial vehicle, or a robotic manipulator.

boundary. Assume that the possible configurations along the planned trajectory at time t are contained in a bounded region $\Omega(q(t)) \subset \mathrm{cl}(\mathcal{C}_{free})$, i.e. $\widetilde{q}(t) \in \Omega(q(t))$. Fig. 1 shows two trajectories q_A and q_B and the associated shaded uncertainty "tubes" along them resulting from the union of all regions $\Omega(q(t))$, for $t \in [0, T]$. The closest points to any obstacle along these trajectories are shown with respective distances d_A and d_B.

Which trajectory should the vehicle select? One choice is to pick a trajectory with maximum distance to the closest obstacle. In Fig. 1 this would be trajectory q_A since $d_A > d_B$. This corresponds to minimizing an L^∞ norm as will be explained in §III. Another choice is a trajectory for which the average closest distance to any obstacle is minimized–which corresponds to an L^1 norm. A third choice is a quadratic penalty for approaching an obstacle defined through an L^2 norm. While such norms account for the spatial properties of the distance-to-obstacle function in this paper we explore more general H^k (for an integer k) Sobolev norms that also capture properties of the function changing with time through its frequency modes representation. Intuitively, the frequency information can be regarded as a global notion about how many times a vehicle approaches obstacles, and how long it remains close to obstacles. Such norms are appropriate for evaluating risk of collision. For instance, as shown in the remaining part of the paper, an H^1 norm can successfully distinguish the de facto safer trajectory q_B unlike standard L^p norms.

II. Safety Metrics

In our setting we define two notions of predicting the safety of a trajectory. The first is the actual expected probability of collision (PC) based on the actual vehicle behavior under all possible environment conditions. Such a probability can be computed by considering all possible scenarios that can happen in the world and computing the fraction of trajectories that collide with obstacles. This would be the ideal metric for evaluating risk. In the absence of precise uncertainty models, an simpler approach is to employ a heuristic metric based solely on a distance-to-obstacle function. Norms based on such function are termed collision avoidance (CA) norms.

We stress that this paper does not propose a new obstacle avoidance scheme. Instead, it is concerned with quantifying more effectively the safest trajectory among a given set of possible actions. For instance, a typical collision handling methods such as dynamic window or potential field (see e.g. [5], [6]) are compatible with such measure by modifying the cost along arcs in the dynamic window, or considering the temporal frequency of the potential, respectively. We demonstrate such ideas through two examples. In essense, this paper attempts to determine which CA norm is most suitable for choosing safer trajectory in real-time. Consequently, the PC norm can be used to evaluate how appropriate this choice was.

A. Approximate Probability of Collision

Probability of collision (PC) can be computed by simulating the vehicle control system, sensing, and external disturbances in a Monte Carlo sampling fashion and computing expected chance of collision. While this is the correct way to compute PC, in this paper we follow a simpler approach which does not require choosing a particular implementation of estimator, trajectory tracking, and collision avoidance controllers. Instead, we assume that the exact nature of uncertainty is unknown but that it is always bounded by a given scalar r, with respect to a given uncertainty metric $\rho : \mathcal{C} \times \mathcal{C} \to \mathbb{R}$, through the operation of the vehicle onboard estimator and controllers.

Under these assumptions we can set

$$\Omega(q) = B^r_\rho(q) \cap \mathrm{cl}(\mathcal{C}_{free}),$$

where the ball with radius r with respect to a metric ρ is defined by $B^r_\rho(q) := \{q' \mid \rho(q, q') < r,\ q' \in \mathcal{C}\}$. Assuming that the vehicle configuration is uniformly distributed (the worst case scenario) within $B^r_\rho(q)$ a simple way to quantify the probability of collision is through the fraction of configurations within the ball that lie inside obstacles. More formally, the probability of collision along trajectory q at time t denoted by $P^c_q(t)$ can be expressed as

$$P^c_q(t) = \frac{\mathrm{vol}\left(\Omega(q(t))\right)}{\mathrm{vol}\left(B^r_\rho(q(t))\right)}. \tag{2}$$

While this notion of probability might seem simplistic and limiting, for the purposes of this paper it is a valid choice since it captures general types of uncertainty and is suitable for verification, for example as used in §IV to evaluate various choices of CA norms.

B. Collision Avoidance Metric

In this paper we use a simple collision avoidance metric based on the inverse of the distance-to-obstacle function $d(q(t))$ defined in (1):

$$f(t) = \begin{cases} \frac{1}{d(q(t))} - \frac{1}{d_0}, & \text{for } d(q(t)) < d_0 \\ 0, & \text{for } d(q(t)) \geq d_0. \end{cases}, \tag{3}$$

where the given scalar d_0 denotes distance to obstacle that poses no danger for collision during execution, or equivalently it satisfies $d(\widetilde{q}(t)) < d_0$, where $\widetilde{q}$ was defined in §I.

This form ensures that $f(t)$ varies smoothly from 0 when far away from obstacles to ∞ at the boundary of the obstacle. It is a standard metric used in robotics. For instance, potential field based obstacle avoidance [7] or trajectory generation using navigation functions [8] are based on scaled and squared versions of (3) (see [3] and [6] for a summary of such methods). Motion planning using trajectory deformation for nonholonomic systems (e.g. [9]) or mobile manipulators (e.g. [10]) are only a few examples among the multitude of work on robotic obstacle avoidance in which (3) appears. Note that often $f(t)$ appears along with a scaling factor which, nevertheless, can be ignored since the norms studied here are scale-invariant.

III. Trajectory Norms

In this section, we first discuss L^p norms on function spaces. We show how these norms can be used to quantify risks of collision and then discuss their shortcomings. We then briefly describe classical Sobolev norms and demonstrate their advantages. A more extensive study of the theory of Sobolev spaces can be found in e.g. [11], [12]. Throughout this section, we will assume any measurability requirement for functions to make the integrals well defined.

A. L^p Spaces

Consider a real valued function $f : \mathbb{R} \mapsto \mathbb{R}$ which maps t to $f(t)$. Then roughly speaking, the p-norm of f denoted by $\|f\|_p$ quantifies the magnitude of a function by combining its height and width. It is formally defined as

$$\|f\|_p = \left(\int |f(t)|^p dt \right)^{1/p}. \tag{4}$$

When $1 \leq p < \infty$, the p-norm of a function is actually a norm satisfying all the three required properties for a norm. It turns out that the space of all measurable functions with finite p-norm forms a Banach space, i.e., a complete normed vector space. This space is denoted by L^p. For the rest of the paper, we use either p-norm or L^p norm to refer to the norm of a function. When $p = 2$, the space L^2 forms a Hilbert space with the inner product $\langle f, g \rangle = \int_{\mathbb{R}} f(x)g(x)dx$. This fact will be used in the next section when we discuss H^k norm of a function.

Example: If f is a step function with height h and width w, the L^p norm of f is $\|f\|_p = |h|w^{1/p}$. When $p = 1$, $\|f\|_1$ is just the total unsigned area enclosed by the graph of f. As $p \to \infty$, the limit norm $\|f\|_\infty$ is just $\sup_{\mathbb{R}} |f(t)|$.

For instance, the maximum value of a function can be extracted using the L^∞ norm. Yet, the L^∞ norm of two functions f and g will be the same even if g achieves its maximum value multiple times. Another observation is that the L^1 norm cannot distinguish between a narrow and tall function and a function whose graph is wide and short since both have equal unsigned area.

We will see in §III-C that such observations have implications in collision avoidance. In the next section, we discuss the classical Sobolev H^k norms, which unlike their L^p counterpart, also take into account the frequency components (or time variations) in a function. This will enable us to develop improved norms quantifying collision risk which we illustrate for an analytical example in §III-C and for a more realistic helicopter dynamics scenario in §IV.

B. Classical H^k Sobolev Spaces

Consider again a real valued function $f : \mathbb{R} \mapsto \mathbb{R}$ which maps t to $f(t)$. We saw in the previous section how L^p norms assign a magnitude to a function based on its height and width. The classical Sobolev norm extends the L^p norm by taking into account not just the height and width but also its derivatives. The classical H^k norm of a function (assuming any measurability and differentiability requirements) is formally defined as

$$\|f\|_{H^k} \equiv \left(\int \sum_{i=0}^{k} \left| \frac{\partial^i f}{\partial t^i} \right|^2 dt \right)^{1/2}, \tag{5}$$

i.e. it consists of sums of the first k derivatives of f squared. The L^2 norm is recovered by choosing $k = 0$. We denote by H^k the space of measurable functions (along with its derivatives) with finite H^k norm. It turns out that the space H^k is also a Banach space. If a function belongs to H^k, then it also belongs to H^m for all $m \leq k$. One can also give a frequency based characterization of H^k norms. If a function belongs to L^2, then it has a well defined Fourier transform[11], again belonging to L^2 and defined as $\hat{f}(\xi) = \int_{\mathbb{R}} f(t)e^{-2\pi i t\xi} dt$. Using Parseval's identity given by $\int_{\mathbb{R}} |f(t)|^2 dt = \int_{\mathbb{R}} |\hat{f}(\xi)|^2 d\xi$, we see that the L^2 norm of a function can also be expressed in term of its Fourier transform. Since the H^k norm is based on the L^2 norm of a function and its derivatives, one can equivalently define it as

$$\|f\|_{H^k} = \left(\int \left(1 + |\xi|^2\right)^k |\hat{f}(\xi)|^2 d\xi \right)^{1/2} \tag{6}$$

When $k = 0$, one recovers the L^2 norm. Using the Fourier characterization of H^k norm, we see that for a function to be in H^k, we require that its Fourier transform decays at a sufficiently fast rate. So in general, a function in H^{k_1} will be "smoother" than a function in H^{k_2} if $k_1 \geq k_2$ if they have comparable norms. Using the Fourier based definition one can also show that H^k in fact is a Hilbert space with inner product $\langle f, g \rangle_k = \int_{\mathbb{R}} \left(1 + |\xi|^2\right)^k \hat{f}(\xi)\overline{\hat{g}(\xi)} d\xi$.

Example: Consider the function $f(t) = h\phi(t/w)\sin(\nu t)$, where $\phi(t)$ is 1 for $|t| \leq w$ and zero elsewhere. This function has height h, width w and frequency ν. The H^1 norm of f is roughly of the order $\|f\|_{H^1} \approx hw^{1/2}\nu$ where as the L^2 is of the order $\|f\|_2 \approx hw^{1/2}$. We see that the L^2 norm is completely oblivious to the frequency component (or time variation) in f. Note that a function could have small height and width but large H^1 norm if it oscillates a lot.

In the next section, the norms introduced in §III-A and §III-B will be used to quantify collision risk for trajectories in an environment with obstacles. We will demonstrate the advantages of Sobolev norms over more traditional norms in the context of the work referred to in §II-B.

C. Analytical Example

In this section, we will discuss what information various norms encode in the context of trajectories in a region with obstacles. Suppose we are given N trajectories $q_i(t), i \in \{1, \ldots, N\}, t \in [0\ T]$ in time and the distance in time information $d(q_i(t))$ of these trajectories to their nearest obstacle (see (1)). How do we quantify the safety of these trajectories based on the collision avoidance function $f(t)$ (see (3)) and choose one with minimal risk? Consider Fig. (2) illustrating $f_i(t)$ for four trajectories labeled by A, B, C, D. The expression for $f_i(t)$ for each of them is

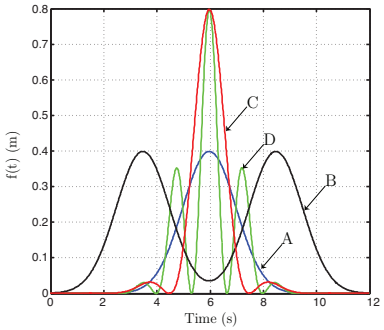

Fig. 2. $f(t)$ versus t plots

TABLE I

TABLE OF VARIOUS SOBOLEV NORMS FOR CURVES IN FIG.2

	L^1	L^2	L^∞	H^1
A	10.0	0.5	0.4	4.2
B	20.0	0.8	0.4	8.4
C	11.1	0.8	0.8	17.5
D	10.0	0.7	0.8	37.8

$$
\begin{aligned}
f_A(t) &= \frac{\exp(-\frac{t^2}{2\sigma^2})}{\sigma\sqrt{2\pi}} \\
f_B(t) &= \frac{\exp(-\frac{(t+2.5)^2}{2\sigma^2})}{\sigma\sqrt{2\pi}} + \frac{\exp(-\frac{(t-2.5)^2}{2\sigma^2})}{\sigma\sqrt{2\pi}} \\
f_C(t) &= \frac{\exp(-\frac{t^2}{2\sigma^2})}{\sigma\sqrt{2\pi}}\,(1+\cos(2\pi\omega_1 t)) \\
f_D(t) &= \frac{\exp(-\frac{t^2}{2\sigma^2})}{\sigma\sqrt{2\pi}}\,(1+\cos(2\pi\omega_2 t))
\end{aligned}
$$

where $\sigma = 1, \omega_1 = \frac{1}{3}, \omega_2 = \frac{3}{4}$. Lets first discuss the qualitative behavior of each of these curves. The curves labeled by A and B correspond to trajectories that lie equally close to an obstacle and so do the curves labeled by C and D. The main difference between curves A, B is that B approaches the minimum distance twice and A just once. Similarly, note that the curves labeled by C, D have the same peak value but the two other peaks for C are lower than those of D and are spread out more than those of D. If one were to visually inspect these curves and sort them in increasing order of risk of collision, one would expect the ordering to be $A \leq B \leq C \leq D$ where $P \leq Q$ means P is safer than Q. Let us see what the L^p and H^k norm tells us about these curves. The various norms for $f_i(t)$ for these four trajectories are listed in Table I. We immediately observe the shortcomings of the L^p norms in this scenario. Lets discus each of these.

a) L^1 norm:: The L^1 norm of $f_i(t)$, containing the average distance of the trajectory from obstacle, gives the ordering $A \leq D \leq C \leq B$. The L^1 cannot differentiate between curves A (narrow and tall) and D (wide and short). But in realistic scenarios with uncertain dynamics, one would want to declare D riskier than A since it approaches obstacles twice as close as compared to A. Thus, the L^1 norm would be a inappropriate choice in terms of quantifying collision risk of a trajectory in an uncertain environment.

b) L^2 norm:: The L^2 norm of $f_i(t)$ gives the ordering $A \leq D \leq B \leq C$. Thus, the L^2 cannot differentiate between curves B and C even though one would want to declare C to be riskier than B since C approaches the obstacles much closer than B. Thus, it is not clear whether L^2 is an appropriate choice for quantifying collision risk.

c) L^∞ norm:: The L^∞ norm of $f_i(t)$, which provides the minimum distance to obstacles gives the ordering $A \leq B \leq C \leq D$. Thus, L^∞ cannot differentiate between curves A and B (and similarly cannot differentiate between curves C and D). This is because the L^∞ does not count how many times a trajectory gets close to an obstacle. In other words, it does not account for frequency in a curve. In realistic scenarios with uncertain dynamics, one would want to choose A over B and C over D. Thus, the L^∞ norm would also be an appropriate choice in terms of quantifying collision risk of a trajectory in an uncertain environment.

d) H^1 norm:: The H^1 norm of $f_i(t)$, which computes the magnitude of $f_i(t)$ based not only the L^2 norm of $f_i(t)$ but also the L^2 of its derivative $\frac{df_i(t)}{dt}$, gives us the the ordering $A \leq B \leq C \leq D$. Thus by using a norm which takes into account the derivative of a function (or its frequency), one is able to construct a collision risk norm whose outcome agrees with our intuition for trajectory safety.

In the next section, we will apply these norms to a semi-realistic helicopter navigating in a cluttered environment and confirm that the H^1 is the optimal choice among the four norms considered.

IV. AERIAL VEHICLE APPLICATION

A. Model

Consider the following model of a small autonomous helicopter depicted in Fig. 3. The vehicle is modeled as a single underactuated rigid body with configuration space $\mathcal{C} = \mathrm{SE}(3)$ described by position $x \in \mathbb{R}^3$ and orientation matrix $R \in \mathrm{SO}(3)$. Its *body-fixed* angular and linear velocities are denoted by $\omega \in \mathbb{R}^3$ and $v \in \mathbb{R}^3$, respectively. The vehicle has mass m and principal moments of rotational inertia J_1, J_2, J_3 forming the inertia tensor $\mathbb{J} = \mathrm{diag}(J_1, J_2, J_3)$.

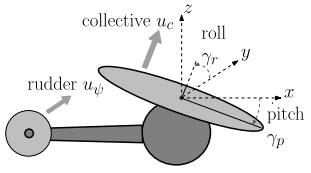

Fig. 3. Simplified helicopter model used in our tests.

The vehicle is controlled through a *collective* u_c (lift produced by the main rotor) and a *yaw* u_ψ (force produced by the rear rotor), while the direction of the lift is controlled by tilting the main blades forward or backward through a *pitch* γ_p and sideways through a *roll* γ_r. The four control inputs then consist of the two forces $u = (u_c, u_\psi)$ and the two shape variables $\gamma = (\gamma_p, \gamma_r)$.

The equations of motion have the standard form (e.g. [13]):

$$\begin{bmatrix} \dot{R} \\ \dot{x} \end{bmatrix} = \begin{bmatrix} R\,\widehat{\omega} \\ R\,v \end{bmatrix}, \tag{7}$$

$$\begin{bmatrix} \mathbb{J}\,\dot{\omega} \\ m\dot{v} \end{bmatrix} = \begin{bmatrix} \mathbb{J}\,\omega \times \omega \\ mv \times \omega + R^T(0,0,-9.81m) \end{bmatrix} + F(\gamma)u, \tag{8}$$

where the map $\widehat{\cdot}: \mathbb{R}^3 \to \mathfrak{so}(3)$ is defined by

$$\widehat{\omega} = \begin{bmatrix} 0 & -\omega^3 & \omega^2 \\ \omega^3 & 0 & -\omega^1 \\ -\omega^2 & \omega^1 & 0 \end{bmatrix},$$

while the control matrix is defined as

$$F(\gamma) = \begin{bmatrix} d_t \sin\gamma_r & 0 \\ d_t \sin\gamma_p \cos\gamma_r & 0 \\ 0 & d_r \\ \sin\gamma_p \cos\gamma_r & 0 \\ -\sin\gamma_r & -1 \\ \cos\gamma_p \cos\gamma_r & 0 \end{bmatrix}.$$

The motion along the trajectories studied next satisfies the dynamics given in (7) and (8).

B. Test scenario

Consider an UAV commanded to fly in minimum time to a given position across a terrain with obstacles. The vehicle has an on-board motion planner which can compute obstacle-free trajectories. While a detailed description of the planning algorithm is not necessary for the purpose of this paper we briefly mention that it is based on a combination of probabilistic roadmaps, trajectory primitives, and dynamic programming [14] and is implemented in C++. Fig. 4 shows five computed trajectories with several states shown to illustrate the vehicle motion.

The terrain is represented using a digital elevation map loaded from a file. The distance $d(q(t))$ between the helicopter trajectory $q(t)$ and the terrain is computed using the Proximity Query Package (PQP) [15] that can compute closest distance between two arbitrary polyhedra.

For simplicity, assume that for obstacle avoidance purposes the helicopter body is represented by a spherical shell with a given radius a, i.e. $\mathcal{A}(q) = B^a(x)$, where $B^a(x) \subset \mathbb{R}^3$ is the sphere with radius a centered at $x \in \mathbb{R}^3$ corresponding to the position coordinates in $q \in \mathcal{C}$. Therefore, uncertainty in the orientation of the helicopter can be ignored and we can assume that the uncertainty in position is bounded by the scalar r (as introduced in §II-A), or equivalently that

$$\rho(q, q') = \|x - x'\| \text{ and } \rho(q, q') < r.$$

Note that in this case the obstacle distance threshold d_0 defined in (3) and r coincide since any distance to obstacle larger than r is considered safe. The ball $B^r_\rho(q(t))$ becomes a regular sphere and the probability of collision at time t along a trajectory $q(t)$ defined in (2) can be computed through its intersection with the terrain.

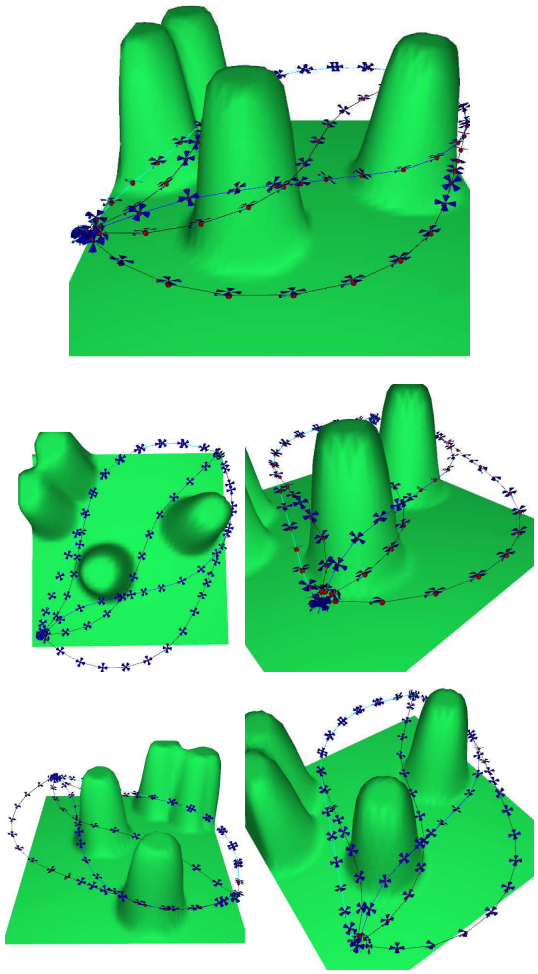

Fig. 4. Helicopter trajectories computed by the on-board motion planner to a given position (five different views shown). These trajectories are of equal cost (final time) but have different probability of collision once executed in the uncertain environment. The tests performed in this section determine which norm is most suitable for predicting and choosing the safest path.

A simple way to perform this computation is to assume some finite discretization using a set of N points $x_i \in B^r(x(t))$ based on which

$$P^c_q(t) \approx \frac{1}{N} \sum_{i=1}^{N} x_i \overset{?}{\in} \mathcal{O}, \tag{9}$$

using the binary notation $a \overset{?}{\in} A \to \{0,1\}$ with $a \overset{?}{\in} A = 1$ only if $a \in A$. The points x_i should be uniformly distributed within B^r, either using a grid or selected in Monte Carlo manner.

The trajectories from Fig. 4 are marked for clarity on Fig. 5. For each trajectory the probability of collision (PC) norms based on the L^1, L^2, L^∞ and H^1 norms of $P^c_q(t)$ and corresponding collision avoidance (CA) norms are computed and shown in Fig. 5. We are interested in determining an appropriate ordering of the trajectories in terms of real risk of collision (computed by PC) and a heuristic notion of safety (computed by CA). The purpose of computing different PC norms is to demonstrate that all PC norms result in identical

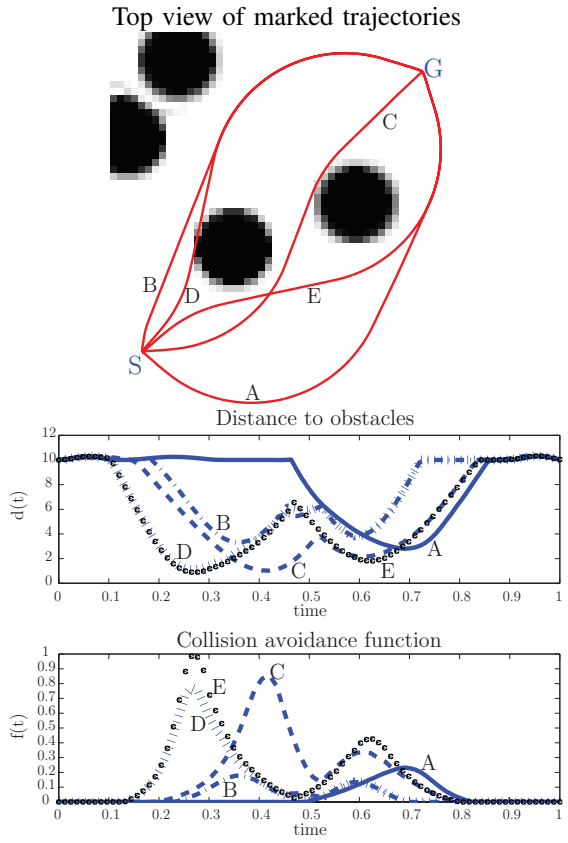

Norm	A	B	C	D	E	Ordering
Probability of Collision Norms						
$\|P_q^c\|_1$	.000	.158	.404	.512	.800	ABCDE
$\|P_q^c\|_2$	.000	.147	.285	.450	.525	ABCDE
$\|P_q^c\|_\infty$	.001	.193	.318	.550	.584	ABCDE
$\|P_q^c\|_{H^1}$	.009	.401	.730	1.041	1.253	ABCDE
Collision Avoidance Norms (f defined in (3))						
$\|f\|_1$	.37	.33	1.13	.97	1.52	BADCE
$\|f\|_2$	.25	.19	.73	.65	.88	BADCE
$\|f\|_\infty$	.23	.18	.84	.76	.98	BADCE
$\|f\|_{H^1}$	.37	.38	1.53	1.28	1.78	ABDCE

Fig. 5. Scenario from Fig. 4 projected onto the $x-y$ plane for clarity (top) followed by the corresponding distance and collision avoidance functions (middle). The computed probability of collision norms (PC) along with the collision norms (CA) of each marked trajectory are given (bottom). All PC norms order the trajectories according to A-B-C-D-E in terms of increasing risk of collision. While all CA norms manage to detect the riskiest trajectory E only the H^1 CA norm manages to extract the correct safest trajectory A.

ordering in terms of increased risk of collision A-B-C-D-E with A being the safest and E the most dangerous trajectory. According to the CA table in Fig. 5 all norms manage to identify the riskiest trajectory E while only the H^1 norm selects trajectory A as the safest trajectory. On the other hand, none of the norms manage to properly order all of the trajectories (H^1 comes closest with A-B-D-C-E). This is due to the fact that all of these norms remain only heuristic and cannot ideally capture the real collision risk. Yet, among the norms considered H^1 appears the most appropriate. As the paper asserts this is achieved through the global frequency component information which it encodes.

V. CONCLUSION AND FUTURE WORK

An interesting extension to the presented work is to consider dynamic obstacles. The nature and magnitude of changes in obstacles can be related to the frequency representation of the distance function to derive more general norms useful for navigation in dynamic environments. When one has deterministic time varying obstacle, the techniques in this paper can be directly applied. What is nontrivial is to develop techniques which can be applied to uncertain obstacles.

REFERENCES

[1] S. M. LaValle, *Planning Algorithms*. Cambridge University Press, Cambridge, U.K., 2006.

[2] S. Thrun, W. Burgard, and D. Fox, *Probabilistic Robotic*. MIT Press, 2005.

[3] J.-C. Latombe, *Robot Motion Planning*. Kluwer Academic Press, 1991.

[4] S. M. LaValle, *Planning Algorithms*. [Online], available at http://msl.cs.uiuc.edu/planning/.

[5] S. Petti and T. Fraichard, "Safe Motion Planning in Dynamic Environments," in *Proc. of the IEEE-RSJ Int. Conf. on Intelligent Robots and Systems*, Edmonton, AB (CA) France, 08 2005, voir basilic : http://emotion.inrialpes.fr/bibemotion/2005/PF05/ address: Edmonton, AB (CA). [Online]. Available: http://hal.inria.fr/inria-00182046/en/

[6] H. Choset, K. M. Lynch, S. Hutchinson, G. A. Kantor, W. Burgard, L. E. Kavraki, and S. Thrun, *Principles of Robot Motion: Theory, Algorithms, and Implementations*. MIT Press, June 2005, iSBN 0-262-03327-5.

[7] O. Khatib, "Real-time obstacle avoidance for manipulators and mobile robots," *International Journal of Robotics Research*, vol. 5, no. 1, pp. 90–98, 1986.

[8] D. E. Koditschek, "Robot planning and control via potential functions," in *The Robotics Review*, J. C. O. Khatib and Lozano-Pérez, Eds. MIT Press, 1989, vol. 1.

[9] F. Lamiraux, D. Bonnafous, and O. Lefebvre, "Reactive path deformation for nonholonomic mobile robots," *IEEE Transactions on Robotics*, vol. 20, no. 6, pp. 967–977, 2004.

[10] O. Brock and O. Khatib, "Elastic strips: Real-time path modification for mobile manipulation," in *Robotics Research*. Springer Verlag, 1998, pp. 5–13.

[11] E. H. Lieb and M. Loss, *Analysis*, 2nd ed., ser. Graduate Studies in Mathematics. Providence, RI: American Mathematical Society, 2001, vol. 14.

[12] L. Hörmander, *The analysis of linear partial differential operators. I*, ser. Classics in Mathematics. Berlin: Springer-Verlag, 2003, distribution theory and Fourier analysis, Reprint of the second (1990) edition [Springer, Berlin; MR1065993 (91m:35001a)].

[13] F. Bullo and A. Lewis, *Geometric Control of Mechanical Systems*. Springer, 2004.

[14] M. Kobilarov, "Discrete geometric motion control of autonomous vehicles," Ph.D. dissertation, University of Southern California, 2008.

[15] S. Gottschalk, M. C. Lin, and D. Manocha, "OBBTree: A hierarchical structure for rapid interference detection," *Eurographics/ACM SIGGRAPH Symposium on Computer Animation*, vol. 30, pp. 171–180.